IEEE Photonics Journal
An IEEE Photonics Society Publication

Open Access

Scattering Loss Estimation Using 2-D Fourier Analysis and Modeling of Sidewall Roughness on Optical Waveguides

Volume 5, Number 3, June 2013

E. Jaberansary
T. M. B. Masaud
M. M. Milosevic
M. Nedeljkovic
G. Z. Mashanovich
H. M. H. Chong

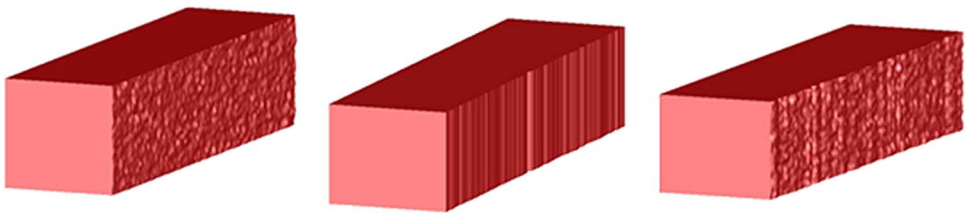

DOI: 10.1109/JPHOT.2013.2251869
1943-0655/$31.00 ©2013 IEEE

IEEE photonics SOCIETY

IEEE

Scattering Loss Estimation Using 2-D Fourier Analysis and Modeling of Sidewall Roughness on Optical Waveguides

E. Jaberansary, T. M. B. Masaud, M. M. Milosevic, M. Nedeljkovic, G. Z. Mashanovich, and H. M. H. Chong

Nano Research Group, Electronics and Computer saience, Faculty of Physical and Applied Sciences, University of Southampton, Southampton SO17 1BJ, U.K.

DOI: 10.1109/JPHOT.2013.2251869

Manuscript received December 17, 2012; revised February 22, 2013; accepted February 26, 2013. Date of publication March 7, 2013; date of current version May 7, 2013. Corresponding author: E. Jaberansary (e-mail: ej08r@ecs.soton.ac.uk).

Abstract: We report an accurate scattering loss 3-D modeling technique of sidewall roughness of optical SOI waveguides based on Fourier and finite-difference time domain (FDTD) analysis methods. The Fourier analysis method is based on the image recovery technique used in magnetic resonant imaging. Losses for waveguides with isotropic and anisotropic roughness are calculated for wavelengths ranging from 1550 to 3800 nm and compared with reported results in literature. Our simulations show excellent agreement with published experimental results and provide an accurate prediction of roughness-induced loss of 3-D arbitrary shaped optical waveguides.

Index Terms: Roughness, scattering loss, optical waveguide.

1. Introduction

Advances in optical waveguide technology allow the integration of optical devices for high performance operations [1]. Semiconductor and dielectric optical waveguides are dominantly considered as the basic building block of complex optical integrated circuits. As the size shrinks down toward nanoscale, some physical waveguide parameters become significant and hence limit the range of operation [2]. The TM mode leakage loss is an example, which can be particularly important for reduced dimensions and certain geometries [3]. One of the other major issues is the radiation loss caused by the scattering of light due to sidewall roughness of the waveguide. Sidewall roughness is a technological process dependent factor. The scattering loss of optical waveguide varies with waveguide geometry, mode polarization state, and roughness parameters. For example, the scattering is more considerable when the optical path is long and also for small and high index contrast waveguides [4]. The effect of scattering on propagation loss in silicon waveguides can be observed in the range from low absorption wavelength region in the near-IR (NIR) to the mid-IR (MIR) wavelength area [5].

The induced loss due to sidewall roughness can be considerably reduced by optimizing the fabrication process [6], [7]. Successful demonstrations show that silicon oxidation can be used to reduce the surface roughness and losses of strip waveguides [6]. This will however change the waveguide cross section dimensions, which are not desirable in precisely designed structures. Atomic layer deposition (ALD) has been recently studied as an alternative [7]. The scattering loss is

considered as an unavoidable feature of nanoscale waveguides and has to be taken into account in the design of photonic elements.

Optical waveguide roughness has been theoretically studied since 1969, when Marcuse established a complete but quite complex analytical expression applicable for 2-D planar waveguides [8]. Payne and Lacey developed a simplified expression by excluding the unnecessary far field term [9]. This expression is hence less complex and includes waveguide physical parameters. It is also commonly accepted as an analytical description for 2-D planar waveguides and widely referred in the literature for comparison with experimental results [4], [10], [11]. There were also attempts to extend Payne and Lacey's model into 3-D structures [12]. However, many of these works have been managed to extend different analytical theories for certain situations and applications (i.e., high or low contrast waveguides and circular waveguides) [13], [14].

In this paper, we report how scattering loss can be accurately estimated from randomly generated roughness on the sidewalls of 3-D optical waveguides. The method to deduce roughness is developed based on an inspiration from the fundamentals of magnetic resonance imaging (MRI) technique [15]. Depending on the fabrication process and anisotropic sidewall roughness, isotropic sidewall roughness is also expected [16]. For a better comparison, the model is therefore designed to accurately implement both types of roughness, making this work distinct from other 3-D waveguide studies where the sidewall roughness is only anisotropic. The model uses two main parameters, which characterize the roughness, i.e., the correlation length and the root-mean-square (RMS) roughness, which is given by a standard deviation from the averaged flat surface. A randomly generated k-space is virtually created in commercial software, Lumerical script environment, which can also be independently executed in any scripting environment. The k-space stores all phase and wavelength information of any surface. It is then filtered according to the real roughness data extracted from atomic force microscopy (AFM) images, and the actual surface is realized by applying the Fourier transform (FT) on the filtered k-space. The generated surface roughness is then implemented as sidewalls of the optical waveguide. With this technique, anisotropic and isotropic sidewall roughness features can be accurately modeled based on surface data extracted from AFM. We use 3-D FDTD technique to estimate the induced loss due to the sidewall roughness of the optical waveguide structure. The accuracy of the loss model is also dependent on the mesh resolution in FDTD. Our final results are compared with other published work.

Our result shows that the model has comparable accuracy to the commonly used scattering loss estimation technique developed by Payne and Lacey [9]. The accuracy can be however improved by using a cluster with more available memory space in order to provide finer mesh settings. Unlike Payne and Lacey's model that is originally developed for sidewalls of 2-D structures, our model can be used for 3-D structures with sidewalls that have anisotropic, isotropic, and mixture of isotropic and anisotropic roughness. Our model can be also implemented on arbitrary waveguide shapes such as cylindrical and triangular geometries and high or low contrast waveguides, where Payne and Lacey's model is not applicable. Roughness can be also deduced on top surface of the waveguide if it is required. In addition, the model can be widely used in any commercial software, using FDTD algorithm in order to estimate the effect of scattering loss for various photonic devices and applications.

2. Generation of Random Roughness on Rectangular Optical Waveguide Sidewalls

The method used to model roughness is based on Fourier analysis approach used in MRI technique [15], [17]. The roughness of a flat surface can be considered as a 2-D image where each point (pixel) has different random correlated intensities. The correlation of these distributed random intensities in the image is defined by a suitable autocorrelation function (ACF). The ACF explains how random variables are related statistically. The ACF of a random roughness is characterized by correlation length L_c and mean-square deviation σ^2 from a flat surface without irregularities. The most commonly used ACFs for process dependent roughness are exponential and Gaussian [9]. AFM measurements of silicon optical waveguide surface roughness have demonstrated that

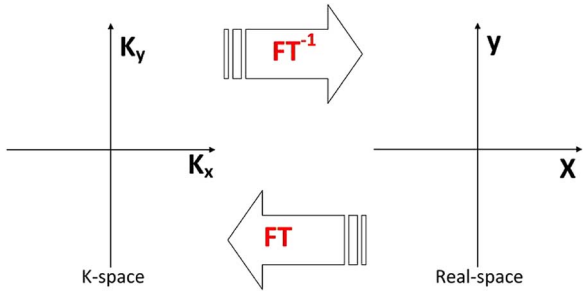

Fig. 1. Real and k-space relation according to Fourier analysis; in the k-space, we express the magnitude, the wavelength, and the phase of all signals that exist in the real image.

Gaussian ACF is a realistic model for the statistics of surface roughness of a variety of waveguides [9]. The Gaussian ACF is expressed as

$$R(u) = \sigma^2 \exp\left(-\frac{u^2}{L_c^2}\right). \tag{1}$$

Here, the image is treated as a random 2-D signal. The Fourier spectrum of this signal is generally represented in a different coordinate, so called k-space. The k-space is a 2-D FT of the original image in real space, as illustrated in Fig. 1. Each point in k-space is a complex number, where its frequency and phase values are obtained in the horizontal and vertical axes, respectively. Hence, it contains all required frequency, phase, and amplitude information of the image in real space and typically has the same number of rows and columns as the original image. Low-frequency components (long wavelengths) are stored around and at the middle and high-frequency components (short wavelengths) near the periphery region. Low spatial frequencies produce only waves with long wavelength characteristics in the original image. These waves only provide contrast information and give little data for the edges. On the other hand, high spatial frequencies eliminate many contrast information in the resultant image, since contrast data are mainly formed by waves only with long wavelength characteristics.

We preferably want to implement the roughness on the sidewalls of a rectangular waveguide. The roughness is initially generated on a flat surface S that is later mapped onto the sidewalls. In order to assign position to different points of the surface S, it has to be mapped in to the real space. At this stage, the surface is considered to be completely flat without having roughness. This means the intensity of all points in the surface is initiated to be zero, and hence, we call it unoccupied real space. In order to expresses our proposed surface S as an unoccupied real space, the surface S is represented by an n by m matrix. The matrix represents surface S is denoted as S_c. The entries of the matrix S_c expresses the position of the associated element in the surface S while the values of the entries express the height level in the surface S. The roughness will be generated above the surface by assigning correlated intensities to the elements of the matrix S_c.

The discrete real space is virtually created by defining two position matrices X and Y that have the same dimension as matrix S_c. This is shown in Fig. 2. They respectively represent x- and y-components of the position vector of each element (point) in the matrix S_c (surface). Hence, any element (intensity) in matrix S_c has an equivalent element in X and Y that specify its position in x- and y-coordinates of the real space.

In this case

$$\begin{aligned} x_{11} &= x_{21} = \cdots = x_{m1} \\ &\vdots \\ x_{1n} &= x_{2n} = \cdots = x_{mn} \end{aligned} \tag{2}$$

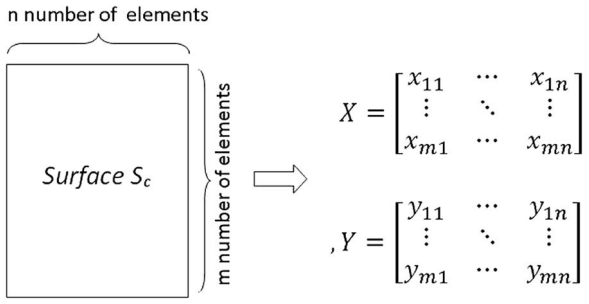

Fig. 2. Creation of discrete real space that contains $n \times m$ elements. X and Y, respectively, store the x and y coordinates of all elements in the surface S_c.

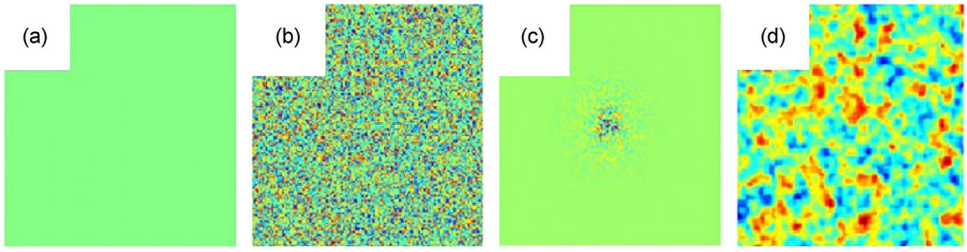

Fig. 3. Generation steps of roughness. (a) Unoccupied k-space: a coordinate showing all available phase and wavelengths for the signals in real image. (b) k-space with randomly generated elements, to include magnitude of each signal. (c) Filtered k-space to remove the edge information. (d) Resulting roughness in real space.

since X only represent the x components of the position vector. For the same reason

$$\begin{aligned} y_{11} = y_{12} = \cdots = y_{1n} \\ \vdots \\ y_{m1} = y_{m2} = \cdots = y_{mn}. \end{aligned} \tag{3}$$

Once the real space is created, the relevant k-space can be also formed. Considering (4) and (5), the required spatial wave vectors $\mathbf{K}_x$ and $\mathbf{K}_y$ of an unfilled k-space associated with the FT of a function of the elements of X and Y is generated. The corresponding k-space is shown in Fig. 3(a), as follows:

$$K_x = \frac{2\pi}{dx \cdot n} x_{nm} \tag{4}$$

$$K_y = \frac{2\pi}{dx \cdot n} y_{nm}. \tag{5}$$

Here, dx represents the spacing between the values of the input x; n and m denote the length of x and y, respectively. In addition, both x and y domain is extended from negative to positive values, and therefore, the generated k-space includes both negative and positive frequencies and phases. When the k-space is constructed, it is filled by uniform random numbers [see Fig. 3(b)]. Each point in k-space has now a random value, which expresses the amplitude of a trigonometric signal at specific frequency and phase. These randomly generated data are stored in a new n by m matrix that is called $\mathbf{Z}$. The matrix $\mathbf{Z}$ is used to express the k-space of the matrix S_c. According to Fourier theory, the superposition of all of the signals stored in $\mathbf{Z}$ will form the final surface S_c. This is where the ACF is used. Applying ACF to the matrix $\mathbf{Z}$ provides a low-pass filter that removes high-frequency components in the k-space, such that the resultant image does not have much of the edge information. This removes the edge details of previously generated uncorrelated random heights. The filtered data are then stored in a matrix called $\mathbf{Z}_{\text{filtered}}$. The resultant K-space, is shown

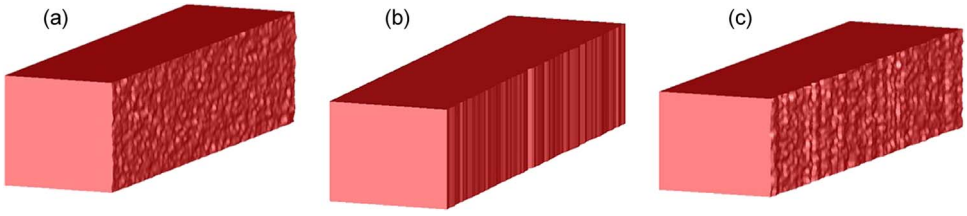

Fig. 4. Different type of roughnesses. (a) Isotropic. (b) Anisotropic. (c) Mixture of isotropic and anisotropic roughness.

in Fig. 3(c). According to (1) the Gaussian ACF is related to the correlation length L_c and mean-square deviation σ^2. Here, sigma σ is defined as:

$$\sigma = Z(n,m) - \frac{\sum_0^n \sum_0^m Z(n,m)}{n \times m}. \tag{6}$$

A certain point at r position in k-space $\sqrt{K_x^2 + K_y^2}$ can be correlated with a point at $r + \sigma$ using (7)

$$Z_{\text{filtered}} = Z(n,m)^2 \times \exp - \left(\sqrt{K_x^2 + K_y^2}/L_c\right)\sigma = Z(n,m) - \frac{\sum_0^n \sum_0^m Z(n,m)}{n \times m}. \tag{7}$$

The resulting values in k-space that are shown in Fig. 3(c) are then transformed back to real space, as can be seen in Fig. 3(d).

Fig. 3(d) shows that the roughness in real space is completely random and characterized to retain the isotropic behavior. Two different randomly generated S_c surfaces can be imported on both sidewalls of a 3-D planar waveguide for further studies on propagation loss characteristics of optical waveguides. Isotropic sidewall roughness and loss analysis has been previously reported in [16]. Accurate AFM/SEM images show that, even on sidewalls with anisotropic roughness, there is still a degree of isotropic roughness features. The difference is illustrated in Fig. 4. Such a characteristic is often ignored in scattering loss evaluations and mathematically reported roughness models.

Isotropic roughness is simply achievable, once the roughness surface in real space is created. In order to generate anisotropic roughness, the following steps are performed. A 1-D random roughness profile is configured by accessing a random row of the matrix that expresses surface S_c. When such a profile is repeated in the y-direction, a new matrix with identical row will be formed. This newly constructed matrix $S_{\text{anisotropic}}$ is used to represent the completely anisotropic surface.

The integration of S_c and $S_{\text{anisotropic}}$ will form the optimal sidewall roughness model that is anisotropic in the y-direction but will still have a level of isotropic behavior. This procedure is shown as follows:

$$\begin{matrix} x_{11} \cdots x_{1n} \\ \vdots \ldots \vdots \\ x_{m1} \cdots x_{mn} \end{matrix} + \begin{matrix} x_{11} \cdots x_{1n} \\ \vdots \ldots \vdots \\ x_{11} \cdots x_{1n} \end{matrix} = \begin{matrix} x_{11} + x_{11} \cdots x_{1n} + x_{1n} \\ \vdots \ldots \vdots \\ x_{m1} + x_{11} \cdots x_{mn} + x_{1n}. \end{matrix} \tag{8}$$

The mixture is formed by superimposing a random $S_{\text{anisotropic}}$ matrix to a random S_c. The matrices $S_{\text{anisotropic}}$ and S_c can have either different or identical roughness properties if required. All three types of roughnesses in Fig. 4 are fully attainable using the same modeling technique. This makes our model reliable and applicable for roughness studies in arbitrary waveguide devices. In addition, the isotropic roughness can be applied on top surface of the waveguide if required.

3. Fabrication and Measurements

Ion bombardment in the dry etch process is considered to be one of the major origins of sidewall roughness. This kind of roughness can be significantly reduced using a low gas pressure and a low radio-frequency power [18], [19]. Pattern transfer during the etch process is also considered as one of the origins of sidewall roughness [19]. We fabricated silicon waveguide structures using

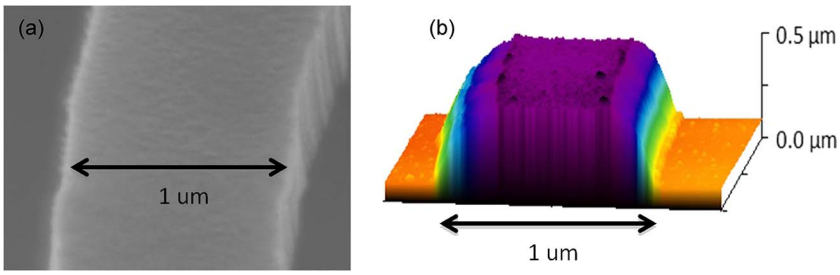

Fig. 5. (a) SEM image of the fabricated waveguide. (b) 3-D AFM view of the fabricated waveguide. The waveguide has 500-nm height and 1000-nm width. The roughness parameters are extracted from the sidewall of this waveguide.

500-nm-thick SOI and 2-μm-thick BOX layer to realize a 500-nm-width waveguide. The other sample contains a 220-nm-wide waveguide on top of the 3-μm BOX layer.

Atomic force microscopic system with special high aspect ratio probe is used to generate multiple AFM images of the optical waveguide. The tip length of the probe is 2 μm and tip radius 10 nm. Fig. 5(b) shows a sample 3-D view of the AFM image of the silicon optical waveguide we have fabricated together with its SEM image. The two main roughness parameters, i.e., RMS and correlation length, are extracted from the edge of sidewalls in the AFM image. The RMS is extracted directly from the profile, and the correlation length is found from the ACF of the profile and equals to the minimum length that makes the normalized autocorrelation minimum ($\approx$zero). The SEM image of the fabricated waveguide is also shown in Fig. 5(a) The reproducible RMS of 5 nm and L_c of 45 nm were obtained from multiple samples.

The dimensions of the waveguides we fabricated are 1000 nm by 500 nm, as shown in Fig. 5. At this dimension, the waveguide can be single mode in the MIR. Once the roughness parameters are extracted from the sidewall of the waveguide, they can be implemented into the simulation model to estimate the scattering loss.

4. Simulations and Discussion

The sidewall roughness parameters of the waveguide are extracted from the AFM measurements and imported to the roughness model, in order to demonstrate the capability of this technique to estimate total scattering loss. In addition to the fabricated waveguide explained above, various waveguides with obtainable roughness features can be also used for the same purpose as will be explained later.

The roughness model has been successfully configured in FDTD Lumerical software package and MATLAB environment. However, in order to run scattering loss simulations of the waveguides, it is preferred to use FDTD Lumerical package because of its particular functionality and supportive features.

The fundamental TE mode is launched into the Si waveguide at a certain wavelength (i.e., 1550 and 3800 nm). Two power monitors record the power transmission data through the waveguide. The first monitor is adjusted at the entry point of the optical waveguide to collect all transmission power information before the light is scattered with generated sidewall roughness. The second one stores these data after 100-μm length. Hence, the scattering loss can be obtained in dB per unit of length.

The calculation of loss using such a method becomes complicated since the problem is numerically very large. A very fine mesh setting is necessary in order to resolve the features on the 3-D waveguide sidewalls. This substantially increases the computational time. In addition, the time-step must be reduced in order to keep within the Courant limit, which makes the calculation time even longer [20]. Although this problem seems to be the major issue to achieve accurate results, tradeoffs in mesh settings can be applied to obtain reasonably accurate results.

We demonstrate the scattering loss by simulating the propagation of light in optical waveguides with the isotropic and anisotropic roughness. Our simulation results are compared with other

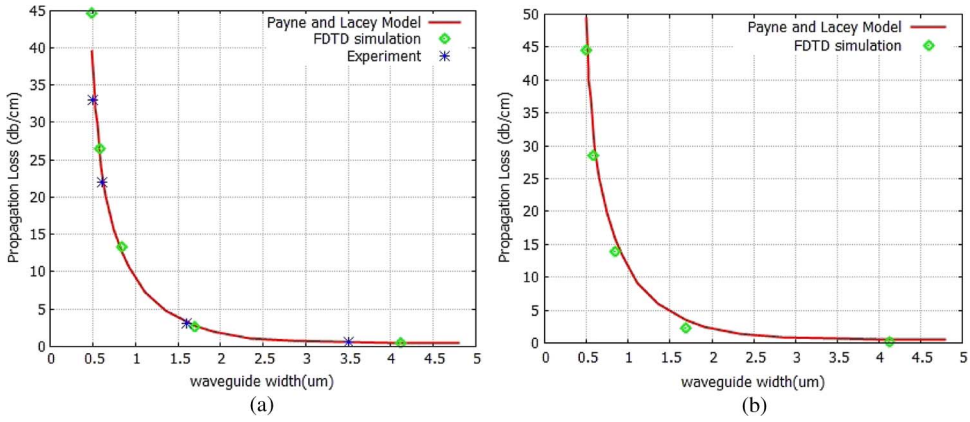

Fig. 6. Comparison of scattering loss of Si waveguides with different widths obtained from [21], Payne and Lacey, and our model for (a) SOI waveguide with a 1-μm deposited layer of SiO_2 added on top of the 0.2 μm and (b) SOI waveguide with no additional SiO_2 layer on top. In both cases, L_c is 50 nm, and σ is 9 nm.

mathematical models and a number of published results. However, the comparison with reported results in literature is difficult since there are various physical parameters that affect the losses. These parameters are mainly related to the cross section of the optical waveguide, the wavelength of light for given dimensions, and also the statistical properties of the sidewall roughness.

We initially investigate the effect of the reduction in waveguide dimensions on the transmission loss. We calculated the transmission loss in three optical waveguides with different sidewall roughness styles. The SOI waveguides have a 200-nm fixed height and width varying from 400 nm to 4.5 μm. These dimensions provides high aspect ratio guide that can help to compare results with estimations obtained by Payne and Lacey's 2-D model [9]. The roughness parameters that are used are $L_c = 50$ nm and $\sigma = 9$ nm. These are the values measured from identical waveguides in [21].

We consider the waveguide in two different situations. First, a deposited 1-μm layer of SiO_2 is added on top of the 0.2-μm SOI waveguide for an accurate comparison to the experimental results obtained in [21]. In the other case, the additional SiO_2 layer is not applied. The effect of size reduction on propagation loss is shown for both cases in Fig. 6(a) and (b), respectively. Here, waveguides have anisotropic rough sidewalls with a level of isotropic behavior. The isotropic statistical components are considered to be five times larger than anisotropic statistical component. Having fully anisotropic sidewall roughness gives identical values to those shown in Fig. 6(a) and (b). However, our other results show that the propagating mode in optical waveguide with completely isotropic sidewall roughness has higher scattering. The loss is as low as 2 dB/cm for waveguide width above 2.5 μm, indicating low scattering losses at the core-cladding interface. However, losses rapidly increase for widths below 2.5 μm and are as high as 44 dB/cm for 300-nm-wide waveguides due to increased interaction between the mode propagating in the waveguide and the sidewalls. Clearly from Fig. 6(a), this is again in excellent agreement with the results reported in [21].

We also use the analytical approach by Payne and Lacey and the following expression to obtain scattering loss [9]:

$$\alpha = 4.34 \frac{\sigma^2}{\sqrt{2} K_0 d^4 n_1} g \cdot f. \tag{9}$$

Here, α is the waveguide scattering loss in dB per unit length, σ is the RMS deviation, k_0 is the free space wave vector, d and n_1 are the waveguide half width and refractive index of Si core, respectively. Function g is determined purely by the waveguide geometry, and f is a function of correlation length and other various parameters defined by Payne and Lacey [9].

In general, the RMS and correlation length of the sidewall roughness can be extracted from the AFM images. The calculated scattering loss based on this approach is also shown in Fig. 6(a) and (b).

TABLE 1

Comparison of the results obtained from our model with a number of experimental or calculated models. The first row corresponds to the waveguide that is shown in Fig. 6, where the data are directly extracted from the AFM image and imported into the Lumerical. The second row is the result for a waveguide with arbitrary dimensions. The other results that are shown here prove the validity of our model as it matches other reported experimental work

Work	Dimension nm×nm (W×H)	Correlation Length(nm)	RMS(nm)	Loss (dB/cm) measured	Loss(dB/cm)- Our Simulations		
					Isotropic	Anisotropic	Mixed isotropic and anisotropic
Our First model (at 1500nm)	330×220	45±5	5±1	33	36.43	29.84	28.65
Our second model (at 3800nm)	1000×500	45±5	5±1	10.2	11.06	10.04	10.53
(1550nm)	445×650	225	5	2.1±0.6	2.6	1.72	1.79
[16](1550nm)	445×220	50	2	3.6±1	5.2	4.5	4.2
[21](1550nm)	500×200	50	9	33	47.32	36.3	36.1
[11](1550nm)	800×1800	225	5	1.1±1	3.30	2.71	2.34
[11](1550nm)	1000×1800	180	9	2.25±0.1	4.2	3.65	3.32
[11](1550nm)	1000×1800	160	13.5	6.5±1.5	9.63	8.94	8.16

As can be seen, the trend of our simulation results is in an excellent agreement with experimental measurements obtained by Lee *et al.* [21] and theatrically estimated by Payne and Lacey. The validity of this trend is completely retained for the uncovered SOI waveguide in Fig. 6(b) and still stays in a good agreement with Payne and Lacey's calculated results. This result shows that, when we have fixed roughness data (RMS and correlation length) and varying geometrical parameter (width or height), comparable estimations can be obtained using either Payne and Lacey [9] or our approach.

From Fig. 6, the interaction of the mode with the sidewalls is strongly enhanced when the waveguide cross section is decreased. Therefore, an accurate comparison can only be possible for optical waveguides with comparable cross sections (comparable propagation constants) and geometry. We use two waveguide samples with two different cross section sizes. The first sample is chosen to be 220 nm by 330 nm in height and width, respectively, while the second one has 1000-nm width and 500-nm height. These dimensions make the cross section of the optical waveguide more identical to other reported works in the literature that we are referring to. The wavelength is again fixed at 1550 nm. In Table 1, our scattering loss simulation results, using the three roughness models, are compared to several published experimental results.

In the second work, we simulate a large waveguide shown in Fig. 5 in MIR wavelength range, at 3.8 μm, where the waveguides operate in single mode. All other dimensions are ranged between 300 and 650 nm in height and 300 and 1000 nm in width. The statistical parameters (RMS and L_c) are process dependent factors, and therefore they vary in a wider range. From Table 1, it can be seen that the simulation results stay in a very good agreement with experimental reported data. It is also important to remember that the loss is measured applying different measurement techniques such as Fabry–Perot or the cutback.

Our AFM measurements show that the anisotropic behavior of the sidewall roughness is more enhanced compared to the isotropic characteristics. In all our samples, the RMS we have measured for anisotropic roughness is at least seven times larger than that for the isotropic roughness of the sidewall surface. This makes the anisotropic component dominant in the mixed case, as can be seen in Table 1. Furthermore, from the data, it seems that anisotropic roughnesses and the mixed isotropic and anisotropic roughnesses more realistically represent the form of actual sidewall roughness, as confirmed by direct measurement of the sidewall roughness.

Based on the data comparison in Table 1 and the discussion on the relationship between the waveguide dimension and the loss, we can extend our model to show the dependence of loss on sidewall roughness parameters for given waveguides. Fig. 7 graphically illustrates the scattering loss dependence on the variation of correlation length when σ is 5 nm. Here, we used a SOI waveguide that is 220 nm by 330 nm in height and width, respectively. This waveguide has relatively low aspect ratio.

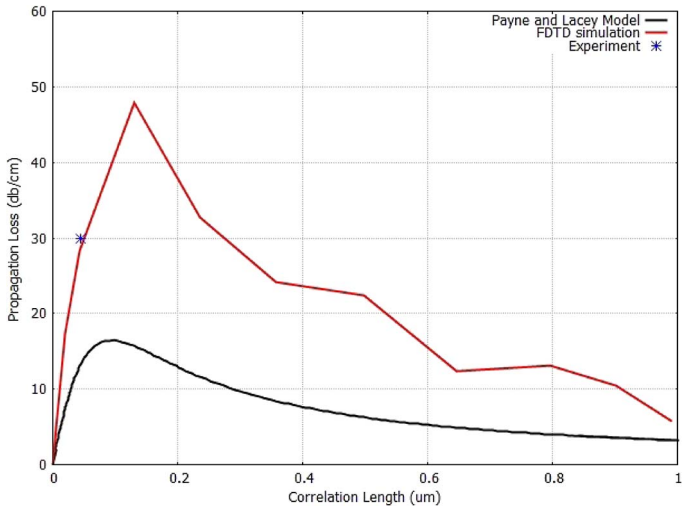

Fig. 7. Propagation loss against the correlation length of the sidewall roughness. Our estimated results is compared with Payne and Lacey's model [10] and our experimental result.

Fig. 7 shows our FDTD simulations in comparison with the predicted results obtained by Payne and Lacey's model [9]. The simulation results show the validity of our experimental data. However, for this relatively low aspect ratio waveguide, Payne and Lacey's estimations do not appropriately match to our FDTD simulations. As expected from the theory [9], when the correlation length of the sidewall roughness is longer than the effective wavelength, the scattering loss is reduced. This is because the variation along the direction of propagation is much larger than the effective wavelength. However, having a very short correlation length causes the waveguide boundary to change very fast. Therefore, the propagating mode cannot determine the details of the sidewall, and consequently, the scattering loss is reduced again. The interaction between the propagating mode and the sidewall roughness is maximized when the correlation length is not very short and very long compared to the effective wavelength.

5. Conclusion

We have successfully demonstrated three types of 3-D sidewall roughness models that are used to analytically estimate the propagation loss in Si photonic waveguides. The simulation results are in excellent agreement with previously published data and Payne and Lacey's analytical method. The main roughness parameters, i.e., correlation length and RMS or standard deviation, are extracted from multiple AFM images of several samples. Using the model, the final scattering loss is calculated and compared for wires with isotropic and anisotropic sidewall roughness. The good agreement between the results proves the applicability of our model for accurate prediction of roughness-induced loss using only three main parameters. We have also shown how our numerical method is valid in different situations such as high and low aspect ratio structures where other analytical model may decline. It is also possible to implement this model into arbitrary waveguide shapes such as cylindrical and triangular geometries, and additional surface roughness can be also deduced on top surface of the waveguide if it is required.

References

[1] G. T. Reed, Ed., *Silicon Photonics—The State of the Art*. Hoboken, NJ, USA: Wiley-Interscience, 2008.
[2] J. P. R. Lacey and F. P. Payne, "Radiation loss from planar waveguides with random wall imperfections," *Proc. Inst. Elect. Eng. J—Optoelectron.*, vol. 137, no. 4, pp. 282–288, Aug. 1990.
[3] M. A. Webster, R. Pafchek, A. Mitchell, and T. Koch, "Width dependence of inherent TM-mode lateral leakage loss in silicon-on-insulator ridge waveguides," *IEEE Photon. Technol. Lett.*, vol. 19, no. 6, pp. 429–431, Mar. 2007.

[4] C. G. Poulton, C. Koos, M. F. Fujii, A. Pfrang, T. Schimmel, J. Leuthold, and W. Freude, "Radiation modes and roughness loss in high index-contrast waveguides," *IEEE J. Sel. Topics Quantum Electron.*, vol. 12, no. 6, pp. 1306–1321, Nov./Dec. 2006.
[5] G. Z. Mashanovich, M. M. Milosevic, M. Nedeljkovic, N. Owens, B. Xiong, E. J. Teo, and Y. Hu, "Low loss silicon waveguides for the mid-infrared," *Opt. Exp.*, vol. 19, no. 8, pp. 7112–7119, Apr. 2011.
[6] D. K. Sparacin, S. J. Spector, and L. C. Kimerling, "Silicon waveguide sidewall smoothing by wet chemical oxidation," *J. Lightw. Technol.*, vol. 23, no. 8, pp. 2455–2461, Aug. 2005.
[7] T. Alasaarela, D. Korn, L. Alloatti, A. Syntjoki, A. Tervonen, R. Palmer, J. Leuthold, W. Freude, and S. Honkanen, "Reduced propagation loss in silicon strip and slot waveguides coated by atomic layer deposition," *Opt. Exp.*, vol. 19, no. 12, pp. 11 529–11 538, Jun. 2011.
[8] M. Marcuse, "Mode conversion caused by surface imperfections of a dielectric slab waveguide," *Bell Syst. Technol. J.*, vol. 48, pp. 3187–3215, Dec. 1969.
[9] F. P. Payne and J. P. R. Lacey, "A theoretical analysis of scattering loss from planar optical waveguides," *Opt. Quantum Electron.*, vol. 26, no. 10, pp. 977–986, Oct. 1994.
[10] K. K. Lee, D. R. Lim, H. C. Luan, A. Agarwal, J. Foresi, and L. C. Kimerling, "Effect of size and roughness on light transmission in a Si/SiO_2 waveguide: Experiments and model," *Appl. Phys. Lett.*, vol. 77, no. 11, pp. 1617–1619, Sep. 2000.
[11] K. P. Yap, A. Delge, J. Lapointez, B. Lamontagne, H. Schmid, P. Waldron, B. A. Syrett, and S. Jan, "Correlation of scattering loss, sidewall roughness and waveguide width in silicon-on-insulator (SOI) ridge waveguides," *J. Lightw. Technol.*, vol. 27, no. 18, pp. 3999–4008, Sep. 2009.
[12] T. Barwicz and H. A. Haus, "Three-dimensional analysis of scattering losses due to sidewall roughness in microphotonic waveguides," *J. Lightw. Technol.*, vol. 23, no. 9, pp. 2719–2732, Sep. 2005.
[13] M. Kuznetsov and H. Haus, "Radiation loss in dielectric waveguide structures by the volume current method," *IEEE J. Quantum Electron.*, vol. QE-19, no. 10, pp. 1505–1514, Oct. 1983.
[14] S. G. Johnson, M. L. Povinelli, M. Solvia Ci, A. Karalis, S. Jacobs, and J. D. Joannopoulos, "Roughness losses and volume-current methods in photonic-crystal waveguides," *Appl. Phys. B Lasers Opt.*, vol. 81, no. 2/3, pp. 283–293, Jul. 2005.
[15] C. Westbrook, C. Kaut Roth, and J. Talbot, *MRI in Practice*. Hoboken, NJ, USA: Wiley, 2011.
[16] Y. Vlasov and S. McNab, "Losses in single-mode silicon-on-insulator strip waveguides and bends," *Opt. Exp.*, vol. 12, no. 8, pp. 1622–1631, Apr. 2004.
[17] W. P. Dong and K. J. Stout, "Two-dimensional fast Fourier transform and power spectrum for surface roughness in three dimensions," *J. Eng. Manuf.*, vol. 209, no. 5, pp. 381–391, Oct. 1995.
[18] E. Z. Liangn, C. J. Huang, and C. F. Li, "Use of SiO_2 nanoparticles as etch mask to generate Si nanorods by reactive ion etch," *J. Vac. Sci. Technol.*, vol. 24, no. 2, pp. 599–603, Mar. 2006.
[19] P. Dumon, W. Bogaerts, V. Wiaux, J. Wouters, S. Beckx, J. Van Campenhout, D. Taillaert, B. Luyssaert, P. Bienstman, D. Van Thourhout, and R. Baets, "Low-loss SOI photonic wires and ring resonators fabricated with deep UV lithography," *IEEE Photon. Technol. Lett.*, vol. 16, no. 5, pp. 1328–1330, May 2004.
[20] S. Kunz and R. J. Luebbers, *The Finite Difference Time Domain Method for Electromagnetics*. Boca Raton, FL, USA: CRC, 1993.
[21] K. K. Lee, D. R. Lim, L. C. Kimerling, J. Shin, and F. Cerrina, "Fabrication of ultralow-loss Si/SiO waveguides by roughness reduction," *Opt. Lett.*, vol. 26, no. 23, pp. 1888–1890, Dec. 2001.